

# Solution Structure of the First Intracellular Loop of Prostacyclin Receptor and Implication of Its Interaction with the C-Terminal Segment of G $\alpha$ s Protein<sup>†</sup>

Lihai Zhang, Jiaxin Wu, and Ke-He Ruan\*

Vascular Biology Research Center and Division of Hematology, Department of Internal Medicine, The University of Texas Health Science Center, Houston, Texas 77030

Received August 5, 2005; Revised Manuscript Received October 20, 2005

**ABSTRACT:** The amino acids (residues 39–51) responsible for the interaction between the first intracellular loop (iLP1) of the human prostacyclin receptor (IP) and G $\alpha$ s protein have been identified [Zhang, L., Huang, G., Wu, J., and Ruan, K. H. (2005) *Biochemistry* 44, 11389–11401]. To further characterize the structural/functional relationship of the iLP1 in coupling with the G $\alpha$ s protein, the solution structures of a constrained peptide (IP iLP1) that mimicked the iLP1 of the IP receptor in the absence and presence of a synthetic peptide, corresponding to the C-terminal 11 residues (Q384–L394 in the protein sequence) of the G $\alpha$ s protein (G $\alpha$ s-Ct), were determined by 2D <sup>1</sup>H NMR spectroscopy. The NMR solution structural model of the iLP1 domain showed two turn structures in residues Arg41–Ala44 and Arg45–Phe49 with the conserved Arg45 at the center. The conformational change of the side chain of the Arg45 was observed upon the addition of the G $\alpha$ s-Ct peptide. On the other hand, the solution structural models of the G $\alpha$ s-Ct peptide in the absence and presence of the IP iLP1 peptide were also determined. The N-terminal domain (Q384–Q390 in the G $\alpha$ s protein) of the peptide adopted an  $\alpha$ -helical conformation. However, the helical structure of the C-terminal domain (Q390–E392 in the G $\alpha$ s protein) of the peptide was destabilized upon addition of the IP iLP1 peptide. These structural studies have implied that there are direct or indirect contacts between the IP iLP1 domain and the C-terminal residues of the G $\alpha$ s protein in the receptor/G protein coupling. The possible charge and hydrophobic interactions between the two peptides were also discussed. These data prompted intriguing speculations on the IP/G $\alpha$ s coupling which mediates vasodilatation and inhibition of platelet aggregation.

Prostacyclin (PGI<sub>2</sub>)<sup>1</sup>, one of prostanoids, is a potent vasodilator and an inhibitor of platelet aggregation, which is mediated by a specific prostacyclin receptor (IP) cloned in 1994 (1). Besides the IP receptor, all of the cloned prostanoid receptors that selectively recognize thromboxane A<sub>2</sub> (TXA<sub>2</sub>) and prostaglandins D<sub>2</sub> (PGD<sub>2</sub>), E<sub>2</sub> (PGE<sub>2</sub>), and F<sub>2</sub> (PGF<sub>2</sub>) (termed TP receptor, DP receptor, EP receptor, and FP receptor) belong to the family of G protein-coupled receptors (GPCRs), which share the seven basic transmembrane domains (TM1–TM7) but couple to different signal transduction systems playing diverse physiological and pathological roles (1–9). The binding of PGI<sub>2</sub> to the IP receptor leads to coupling with Gs, a G protein that couples to adenylyl cyclase, and results in a subsequent elevation

of intracellular cAMP levels. The knowledge of the precise interaction between the IP receptor and Gs protein is crucial in the understanding of the action mechanism of pathophysiological processes of the IP receptor.

The Gs protein interacts with the intracellular domains of GPCR in a multisite fashion with a major contact at the carboxyl terminus of its G $\alpha$  subunit (G $\alpha$ s; 10). Several other segments along the sequence of the G $\alpha$ s are also found to be involved in the selectivity of Gs activation by the particular GPCR (11). The crystal and NMR solution structures of the parts of the G $\alpha$ s protein including the C-terminal segment are now available (12–17). Unfortunately, it is clear that detailed knowledge of the IP/Gs interaction cannot be reliably obtained from the structures of the G $\alpha$ s protein alone due to the lack of a 3D structure of the IP receptor. However, spectroscopic investigations of synthetic peptides consisting of receptor fragments provided a method for identification of the structural and functional features of the loops of the GPCRs, and this method has been widely used (18, 19). By the combination of NMR spectroscopy and site-directed mutagenesis, we have solved several loop structures for the TP (20–22) and IP (23) receptors, which have allowed us to gain insight into the molecular mechanisms of ligand recognition and G protein coupling for the receptors.

Recently, we have analyzed a constrained peptide that mimicked the iLP1 domain of the IP receptor using NMR

<sup>†</sup> This work was supported by NIH Grants HL56712 and HL079389 (to K.-H.R.).

\* To whom correspondence should be addressed. Tel: 713-500-6769. Fax: 713-500-6810. E-mail: kruan@uth.tmc.edu.

<sup>1</sup> Abbreviations: dd water, deionized distilled water; IP, prostacyclin (prostaglandin I<sub>2</sub>) receptor; TP, thromboxane A<sub>2</sub> receptor; EP, prostaglandin E<sub>2</sub> receptor; DP, prostaglandin D<sub>2</sub> receptor; FP, prostaglandin F<sub>2</sub> receptor; IP iLP1, the first intracellular loop of the IP receptor; IP-wt, wild-type IP receptor; G protein, guanine nucleotide binding protein; G $\alpha$ s,  $\alpha$  subunit of the heterotrimeric G protein complexes which activate adenylyl cyclase; TM, transmembrane domain; NMR, nuclear magnetic resonance; DQF-COSY, double-quantum-filtered correlation spectroscopy; TOCSY, total correlation spectroscopy; NOESY, nuclear Overhauser effect spectroscopy; PGI<sub>2</sub>, prostaglandin I<sub>2</sub>; HPLC, high-performance liquid chromatography; hCys or hC, homocysteine.

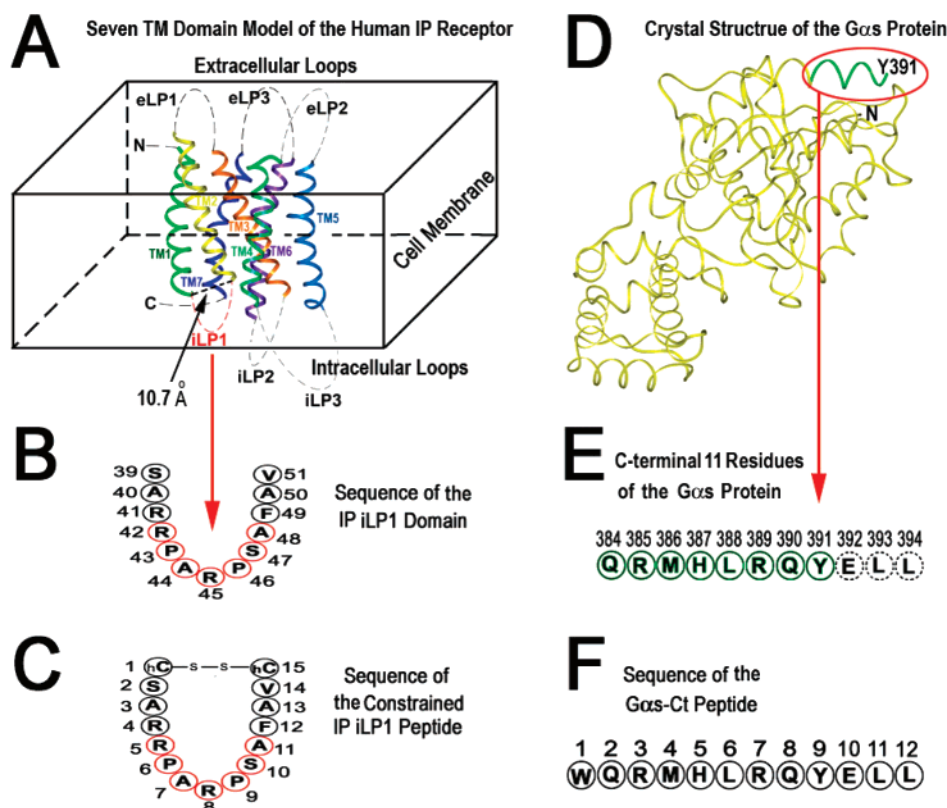


**FIGURE 1:** Sequences of synthetic peptides that mimicked human IP iLP1 and the C-terminal segment of G $\alpha$ s protein. (A) A seven transmembrane (7TM) domain model of human IP receptor (23). The blue straight dashed line denotes the 10.7 Å distance of the TM1 and TM2 of the IP receptor working model generated on the basis of bovine rhodopsin (23). The elliptical dashed lines denote the undefined structures of the first (iLP1, red), second (iLP2, gray), and third (iLP3, gray) intracellular loops. (B) Amino acid sequence of the first intracellular loop (iLP1) of IP receptor. (C) Amino acid sequence of the constrained IP iLP1 peptide with a disulfide bond connecting the added hCys residues at the C- and N-termini. The position of the seven residues involved in the IP signaling identified previously (24) are also highlighted in the red circle in panels B and C. (D) Crystal structure of the human G $\alpha$ s protein. Residues Q384–Y391 are indicated in a solid green rectangular ribbon. The locations of the N-terminus (N) and residue Y391 in the C-terminus are also indicated, but N-terminal residues 1–33 and C-terminal residues 392–394 are disordered and not shown in the crystal structure (14). (E) Amino acid sequence of the C-terminal 11 residues of the G $\alpha$ s protein in the crystal structure. The ordered residues shown in the crystal structure Q384–Y391 are indicated with green circles, and the disordered residues E392–L394 are also indicated in dashed black circles. (F) Amino acid sequence of the G $\alpha$ s-Ct peptide (corresponding to the G $\alpha$ s C-terminal 11 residues) with an additional Trp residue (W1) providing the fluorescence signal.

spectroscopy and site-directed mutagenesis and identified seven residues in the iLP1 domain important to the G $\alpha$ s-mediated signaling (24). In addition, we have observed several residues in the C-terminal segment of the G $\alpha$ s in contact with the IP iLP1 in the 2D NMR spectra (24). In this paper, to further characterize the structure/function relationship of the IP/Gs-mediated signaling, we described 3D NMR structures of the IP LP1 and G $\alpha$ s-Ct peptides and their interaction in solution. The structural studies revealed the molecular mechanisms of the contacts in this peptide–peptide interaction and provided an implication for the receptor/Gs protein coupling at the residue level with 3D structural properties.

## EXPERIMENTAL PROCEDURES

**Materials.** Ethanol- $d_6$  and D $_2$ O were purchased from Cambridge Isotope Laboratories, Inc. (Andover, MA), and trifluoroacetic acid (TFA) was obtained from Millipore (Bedford, MA).

**Peptide Synthesis.** The procedures of the peptide syntheses were the same as previously described (24). The constrained loop peptide that mimicked the sequence of the putative IP iLP1 (residues 39–51) with homocysteine (hCys) residues

added at both ends was synthesized by the fluorenylmethoxycarbonyl-polyamide solid phase method and constrained by the formation of disulfide bond. In addition, the G $\alpha$ s-Ct peptide that mimicked the sequence of the C-terminal region (residues 384–394) of the G $\alpha$ s protein, with a Trp residue added at the N-terminus, was also synthesized and purified by HPLC.

**NMR Sample Preparation.** For 2D NMR spectroscopic studies, the peptide sample of the HPLC-purified constrained IP iLP1 peptide or G $\alpha$ s-Ct peptide was dissolved in 0.5 mL of sodium phosphate buffer (20 mM, pH 6.0), which contained 10% D $_2$ O and 5% ethanol- $d_6$ , with a final concentration of 5.4 or 8.4 mM, respectively. The concentration of IP iLP1 peptide and G $\alpha$ s-Ct peptide in the mixture was also 5.4 and 8.4 mM, respectively.

**NMR Experiments.** Proton NMR experiments were carried out on a Bruker AMX-600 spectrometer. Two-dimensional  $^1$ H NMR experiments including DQF-COSY, TOCSY, and NOESY were performed for the IP iLP1 peptide, the G $\alpha$ s-Ct peptide, or their mixture at 298 K. The WATERGATE method was used to suppress the signal of water. NOESY spectra were recorded with a mixing time of 200 ms. TOCSY spectra were carried out with decoupling in the presence of

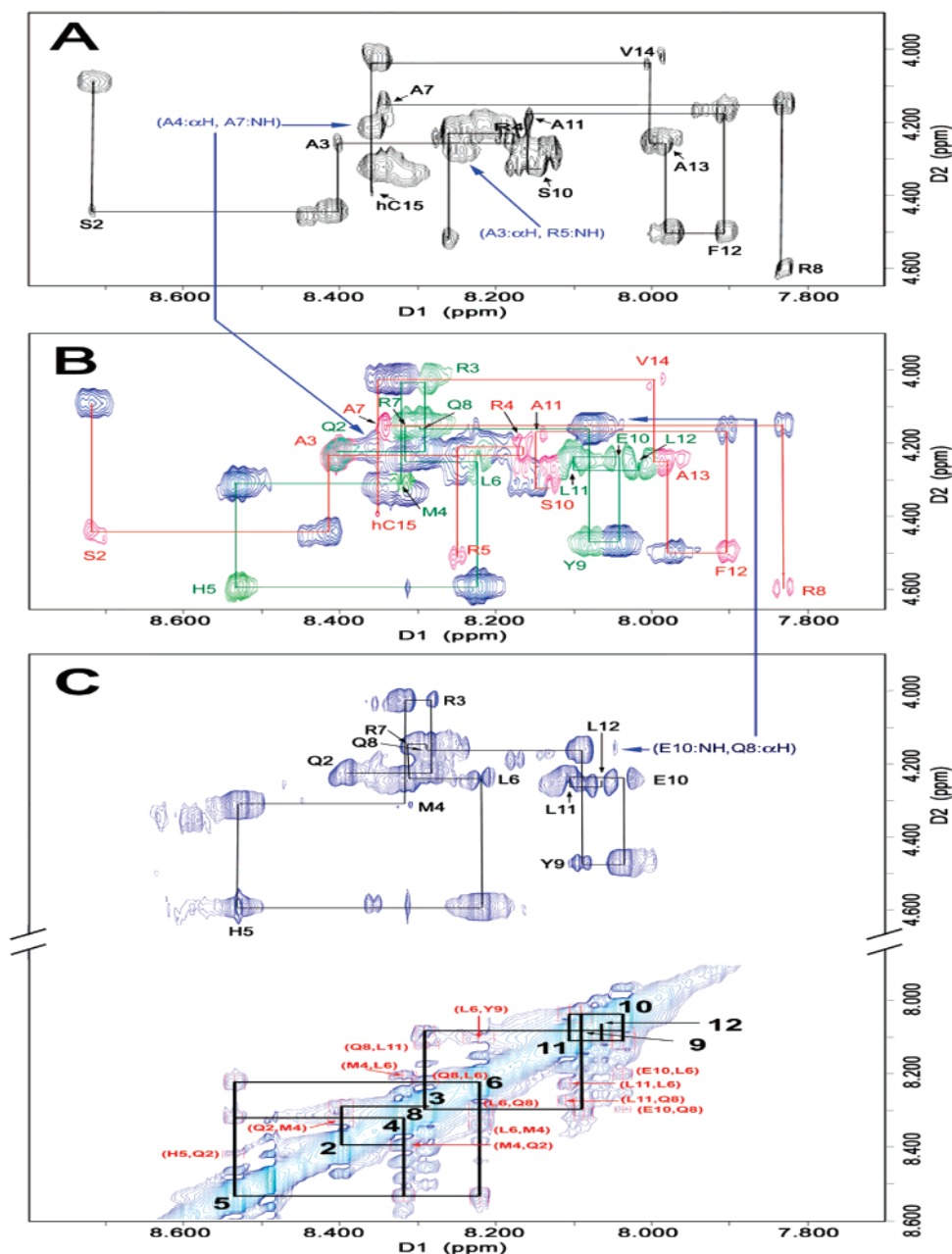


FIGURE 2: Contour plot of the expanded  $\alpha\text{H}$ –NH regions of the 600 MHz NOESY spectra (200 ms mixing time). The amino acid residues (given in single-letter amino acid notation) and numbering within the peptide are shown. The assignments for medium-range cross-peaks were indicated by the red or blue letters in parentheses. (A) Pathway of sequential assignments via  $d_{\alpha\text{N}}$  for the IP iLP1 peptide (5.4 mM). (B) Pathways of sequential assignments via  $d_{\alpha\text{N}}$  for the mixture of the IP iLP1 peptide (5.4 mM) and the  $\text{G}\alpha\text{s}$ -Ct peptide (8.4 mM). The intraresidue cross-peaks of the IP iLP1 and the  $\text{G}\alpha\text{s}$ -Ct peptides are indicated in red and green, respectively. (C) Pathway of sequential assignments via  $d_{\alpha\text{N}}$  for the  $\text{G}\alpha\text{s}$ -Ct peptide (8.4 mM). The  $d_{\text{NN}}$  (in red parentheses) and some other NOE connectivities in these regions are also indicated.

the scalar interaction spin-lock sequence with a total mixing time of 50 ms. A total of 512  $t_1$  increments were used in  $F_1$  with 32 scans per  $t_1$  increment and were composed of 2048 complex points in  $F_2$  in all experiments. Quadrature detection was achieved in  $F_1$  by the States time-proportional phase increment 150 zero-filled to  $2048 \times 2048$  before Fourier transformation, and a  $0^\circ$  (for DQF-COSY) or  $90^\circ$  (for TOCSY and NOESY) shifted sinebell2 window function was used in both dimensions. The ethanol- $d_6$  peak was used as the reference for chemical shifts. The chemical shift and sequence-specific assignments were obtained using standard methods (25) and autoassignment software (26).

**Calculation of Structures.** The overall structure of the peptide was determined through the utilization of intra-

residue, sequential, and medium-range NOEs. The Felix2000 program was used for quantification of the NOE cross-peak volumes and for converting them into upper bounds of the interproton distances. NOE cross-peaks were segmented using a statistical segmentation function and characterized as strong, medium, and weak, corresponding to upper bound distance range constraints of 2.5, 3.5, and 6.0 Å, respectively. Lower bounds between nonbonded atoms were set to the sum of their van der Waals radii (approximately 1.8 Å). Pseudoatom corrections were added to interproton distance restraints where necessary (27). Distance geometry calculations were carried out on an SGI workstation using DGII and NMR refinement programs within the Insight II package (Accelrys, San Diego, CA). NOE constraints and torsion



angle restraints that were derived from coupling constants were used for the initial structure calculation using the DGII program. Energy refinement calculations, including restrained minimization/dynamics, were carried out in the best distance geometry structures using the Discover programs within the Insight II package.

## RESULTS

*Synthesis and NMR Assignment of a Constrained Peptide That Mimics the IP iLP1 Domain and a Linear Peptide That Mimics the C-Terminal Segment of the G $\alpha$ s Protein.* The distance between the  $\alpha$  carbon (C $\alpha$ ) atoms of the two residues (Leu38 in TM1 and Leu52 in TM2 at the intracellular ends) flanking the N- and C-termini of the IP iLP1 is in a range of 10–12 Å with an average of 10.7 Å (Figure 1A). The partially characterized peptide corresponding to the human IP iLP1 domain with a constrained N- and C-terminal distance of approximately 10–12 Å by the addition of a homocysteine disulfide bond described in the previous studies (24, Figure 1C) was continuously used for the solution structural studies. On the other hand, the peptide and minigene studies identified that the C-terminal 11 residues of the G $\alpha$ s protein could interact directly with many GPCRs (28–31). Thus, a synthetic peptide, G $\alpha$ s-Ct, corresponding to the C-terminal 11 residues of the G $\alpha$ s protein as well as an additional Trp residue at the N-terminal position (providing easier identification of the conformational change signals in fluorescence studies, Figure 1D–F) described in the previous studies was adopted for the studies of its solution structure and its interaction with the IP iLP1 domain in solution.

*Evidence of the IP iLP1 Domain and the C-Terminal Segment of the G $\alpha$ s Protein Involved in Receptor Signaling through IP/G $\alpha$ s Coupling.* Residues 42–48 in the IP iLP1 domain involved in the IP signaling through G $\alpha$ s protein coupling have been identified by site-directed mutagenesis experiments (24). Residues Arg42, Ala44, and Arg45 in the IP iLP1 domain and Tyr391–Leu394 in the G $\alpha$ s C-terminal segment important to the IP/G $\alpha$ s contact were also predicted by the chemical shift perturbation approach using the constrained IP iLP1 peptide and the G $\alpha$ s-Ct peptide (24). On the basis of these studies, further characterization of the solution structures of the IP iLP1 and G $\alpha$ s-Ct peptides will give more detailed information for understanding the molecular mechanisms of the IP/G $\alpha$ s coupling in structural terms and provide insights to characterize the structural and functional relationship for the signaling of the GPCR family in general.

*Secondary Structure of the Constrained IP iLP1 Peptide Identified by 2D  $^1\text{H}$  NMR Spectroscopy.* Two-dimensional NMR spectra of the constrained IP iLP1 peptide were recorded in H<sub>2</sub>O, and  $^1\text{H}$  NMR assignments were accomplished using the standard sequential assignment technique. The procedures involved the identification of spin systems and sequential assignment using a combination of TOCSY, DQF-COSY, and NOESY (Figure 2A,B) spectra for the IP iLP1 peptide in the absence (Figure 2A) and the presence (Figure 2B) of the G $\alpha$ s-Ct peptide. The complete proton resonance assignments for the peptide are summarized in Table 1. To find out specific NOEs for the determination of the secondary structures of the peptides in solution,

Table 1: Proton Resonance Assignment (in ppm) for the Constrained IP iLP1 Peptide in the Absence and Presence (in Bold If Different) of the G $\alpha$ s-Ct Peptide

residue	NH	$\alpha\text{H}$	$\beta\text{H}$	$\gamma\text{H}$	others
hCys1		4.092	2.245, 2.233	2.740, 2.721	
Ser2	8.713	4.446	3.815, 3.788		
Ala3	8.401	4.262	1.310		
Arg4	8.164	4.227	1.719, 1.645	1.555, 1.511	$\epsilon\text{H}$ 7.091; $\delta\text{CH}_2$ 3.096, 3.096
Arg5	8.250	4.519	1.745, 1.640	1.588, 1.579	$\epsilon\text{H}$ 7.113; $\delta\text{CH}_2$ 3.110, 3.110
	<b>8.245</b>				
Pro6		4.331	2.201, 1.856	1.920, 1.906	$\delta\text{CH}_2$ 3.716, 3.535
Ala7	8.342	4.152	1.325		
		<b>4.157</b>			
Arg8	7.825	4.598	1.762, 1.637	1.549, 1.538	$\epsilon\text{H}$ 7.109; $\delta\text{CH}_2$ 3.140, 3.131
	<b>7.828</b>				<b>3.146, 3.137</b>
Pro9		4.271	2.216, 1.868	1.985, 1.916	$\delta\text{CH}_2$ 3.698, 3.566
Ser10	8.128	4.313	3.852, 3.752		
Ala11	8.145	4.174	1.192		
Phe12	7.900	4.504	3.099, 2.900		$\epsilon$ (3,5) 7.284; $\zeta$ (4) 7.229; $\delta$ (2,6) 7.167
Ala13	7.971	4.244	1.265		
Val14	7.989	4.024	2.020	0.891, 0.871	
hCys15	8.342	4.384	2.172, 2.025	2.746, 2.649	

surveys of the sequential and medium-range NOEs and the spin–spin coupling constants of the peptides were shown in Figure 3. The lack of the medium-range NOEs for specific  $\alpha$ -helical structure (such as  $d_{\text{NN}(i,i+2)}$ ,  $d_{\alpha\beta(i,i+3)}$ , and  $d_{\text{NN}(i,i+4)}$ ) in NOESY spectra (Figure 3) suggests that the peptides do not contain helical conformation.

The presence of the NOEs of  $d_{\alpha\text{N}(i,i+2)}$  and  $d_{\alpha\text{N}(i,i+3)}$  in the NOE spectra (Figure 3) suggests potential turn structures in residues Arg4–Ala7 of the peptides in solution, which correspond to Arg41–Ala44 in the IP receptor. Besides the secondary structure specific NOEs, other sequential and medium-range connectivities will help to generate constraints to build general conformations for the peptides. A total of 185 distance restraints (140 intraresidue, 40 sequential, and 5 medium-range restraints) were obtained for the IP iLP1 peptide in the absence of the G $\alpha$ s-Ct peptide (Figures 3A and 4A), and a total of 177 distance restraints (136 intraresidue, 37 sequential, and 4 medium-range restraints) were obtained for the IP iLP1 peptide in the presence of the G $\alpha$ s-Ct peptide (Figures 3B and 4B). In addition, 11 dihedral angles were obtained from the DQF-COSY spectra for the IP iLP1 peptides (Figure 3).

*Secondary Structure of the G $\alpha$ s-Ct Peptide Identified by 2D  $^1\text{H}$  NMR Spectroscopy.* Two-dimensional NMR spectra, TOCSY, DQF-COSY, and NOESY (Figure 2B,C) of the G $\alpha$ s-Ct peptide in the absence (Figure 2C) and the presence (Figure 2B) of the IP iLP1 peptide were recorded in H<sub>2</sub>O, and  $^1\text{H}$  NMR assignments were accomplished as described above. The complete proton resonance assignments for the peptides are summarized in Table 2. To find out specific NOEs for the determination of the secondary structures in the peptides, surveys of the sequential and medium-range NOEs and the spin–spin coupling constants of the peptide were shown in Figure 5. Abundant medium-range distances,  $d_{\text{NN}}$  and  $d_{\alpha\text{N}}$ , were identified through the entire sequence of the peptide in the absence of the IP iLP1 peptide, indicating the presence of an  $\alpha$ -helical conformation of the G $\alpha$ s-Ct

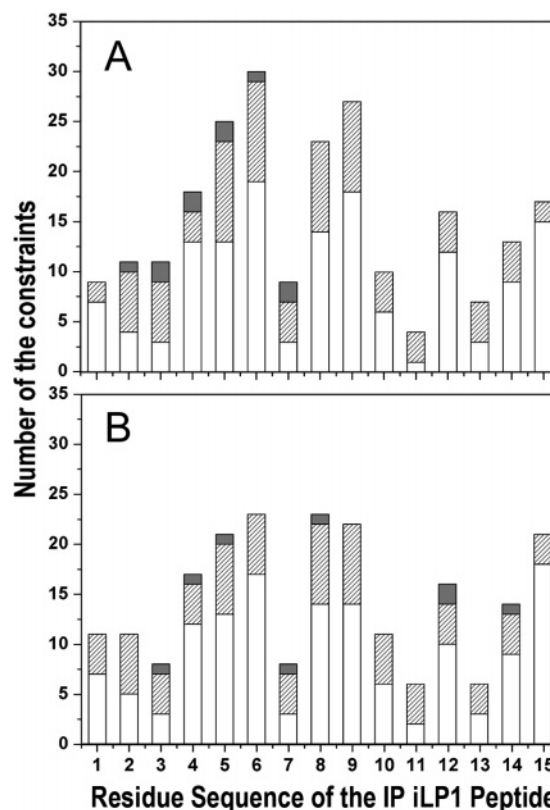


FIGURE 4: Number of constraints per residue for the IP iIP1 peptide in the absence (A) and presence (B) of the G $\alpha$ s-Ct peptide. Intraresidue, sequential, and medium-range NOEs are shown as white, hatched, and filled bars, respectively.

FIGURE 3: Amino acid sequence of the IP iLP1 peptide and a survey of sequential and medium-range NOE constants of the peptide in the absence (A) and presence (B) of the Gas-Ct peptide. At the top of each panel, the residues within the peptide are indicated in single-letter amino acid notation, and their numbering from the IP iLP1 peptide and corresponding numbering from the IP receptor are also indicated. Sequential and medium-range NOEs are indicated by lines starting and ending at the position of the interaction residues. The values of the  $^3J_{\text{NH}\alpha}$  coupling constants are reported as strong ( $J > 7$  Hz; s), medium ( $J = 5-7$  Hz; m), or weak ( $J < 5$  Hz; w), respectively. At the bottom of the panels, the locations of turn structures are shown.

peptide in solution (Figure 5A). Upon addition of the IP iLP1 to the G $\alpha$ s-Ct peptide in solution, several  $\alpha$ -helical structure related NOEs were significantly reduced (such as  $d_{NN(i,i+3)}$ ,  $d_{NN(i,i+4)}$ , and  $d_{NN(i,i+5)}$ ) in the range of the C-terminal segment (Q8–L11) of the G $\alpha$ s-Ct peptide (Figure 5B). This information strongly suggested the presence of conformational changes of the G $\alpha$ s-Ct peptide in these C-terminal residues upon its interaction with the IP iLP1 peptide in solution. In contrast, the  $\alpha$ -helical structure related NOEs in the N-terminal segment of the G $\alpha$ s-Ct peptide were unchanged (Figure 5B). On the basis of the assignment of the NOESY spectra, a total of 182 distance restraints (131 intraresidue, 41 sequential, and 10 medium-range restraints) were obtained for the G $\alpha$ s-Ct peptide in the absence of the IP iLP1 peptide (Figures 5A and 6A), and a total of 182 distance restraints (129 intraresidue, 41 sequential, and 12 medium-range restraints) were obtained for the G $\alpha$ s-Ct peptide in the presence of the IP iLP1 peptide (Figures 5B and 6B). In addition, 11 dihedral angles were obtained from the DQF-COSY spectra for the G $\alpha$ s-Ct peptides (Figure 5).

Table 2: Proton Resonance Assignment (in ppm) for the Gαs-Ct Peptide in the Absence or Presence (in Bold If Different) of the IP iLP1 Peptide

residue	NH	$\alpha$ H	$\beta$ H	$\gamma$ H	others
Trp1		4.236	3.312, 3.283		2H, 7.224; 4H, 7.460; 5H, 7.046; 6H, 7.153; 7H, 7.419; indole, 10.149
Gln2	8.400	4.224	1.932, 1.816	2.182, 2.182	
Arg3	8.286	4.033	1.661, 1.628	1.497, 1.497	$\epsilon$ H 7.103; $\delta$ CH <sub>2</sub> 3.078
Met4	8.316	4.318	1.873, 1.858	2.453, 2.397	
His5	8.528	4.592	3.143, 3.072		2H, 7.828; 4H, 7.278
Leu6	8.217	4.244	1.479, 1.471	1.532	$\delta$ CH <sub>3</sub> 0.831, 0.779
Arg7	8.315	4.154	1.666, 1.649	1.515, 1.475	$\epsilon$ H 7.077; $\delta$ CH <sub>2</sub> 3.088
Gln8	8.289	4.158	1.864, 1.852	2.122, 2.087	
Tyr9	8.087	4.477	2.963, 2.863		$\delta$ (2,6) 7.014; $\epsilon$ (3,5) 6.719
	<b>8.075</b>				
Glu10	8.037	4.246	1.950, 1.848	2.274, 2.274	
	<b>8.040</b>			<b>2.271, 2.271</b>	
Leu11	8.103	4.266	1.532, 1.532	1.532	$\delta$ CH <sub>3</sub> 0.851, 0.798
	<b>8.097</b>				<b>0.848, 0.795</b>
Leu12	8.062	4.244	1.556, 1.556	1.556	$\delta$ CH <sub>3</sub> 0.833, 0.781
	<b>8.012</b>	<b>4.259</b>	<b>1.550, 1.550</b>		<b>0.830, 0.778</b>

*Description of the 3D Structural Models of the IP iLP1 Domain.* On the basis of NOE constraints and dihedral angles, 100 first-generation structures for the IP iLP1 peptide in the absence and the presence of the G $\alpha$ s-Ct peptide were obtained using a DGII program calculation. The constraints

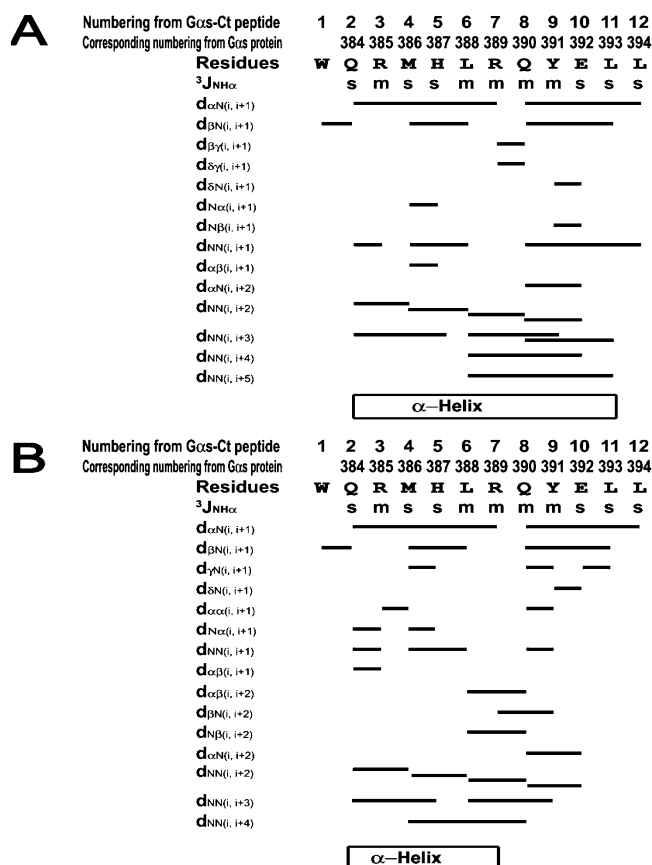


FIGURE 5: Amino acid sequence of the Gαs-Ct peptide and a survey of sequential and medium-range NOE HN–Hα coupling constants of the peptide in the absence (A) and presence (B) of the IP iLP1 peptide. At the top of each panel, the residues within the peptide are indicated in single-letter amino acid notation, and their numbering from the Gαs-Ct peptide and corresponding numbering from the Gαs protein are also indicated. Sequential and medium-range NOEs are indicated by lines starting and ending at the position of the interaction residues. The values of the  $^3J_{\text{NH}\alpha}$  coupling constants are reported as strong ( $J > 7$  Hz; s), medium ( $J = 5$ –7 Hz; m), or weak ( $J < 5$  Hz; w), respectively. At the bottom of the panels, the locations of α-helical structures are shown.

used for the structural calculations of the IP iLP1 peptide in the absence and presence of the Gαs Ct peptide are displayed in Figure 7A,B. Ten selected structures have backbone RMSD values of  $1.2 \pm 0.1$  Å for Ala3–Arg8 and  $1.8 \pm 0.3$  Å for Pro9–Ala13 (data not shown). Energy refinement calculations (minimization/dynamic) were then carried out on the basis of the best distance geometry structures using a Discover program within the Insight II package. Eleven structures were obtained and superimposed as shown in Figure 7C,D, in which the backbone RMSD values of the structures were reduced to  $0.8 \pm 0.2$  Å. The final structure clearly showed a loop structure with two-turn conformation that has Arg8 (corresponding to Arg45 in the IP receptor) in the center. The first turn was in residues Arg4–Ala7 (corresponding to Arg41–Ala44 in the IP receptor) which matched the structural prediction from the NOE survey data (Figure 3). The second relatively loose turn was observed in residues Arg8–Phe12 (corresponding to Arg45–Phe49 in the IP receptor), which was mainly formed by the sequential and medium-range distance constraints (Figure 7A,B). The distance between the N- and C-termini of the iLP1 peptide structures in both forms is approximately 11 Å (Figure 7C,D). The Cα atoms used in obtaining this

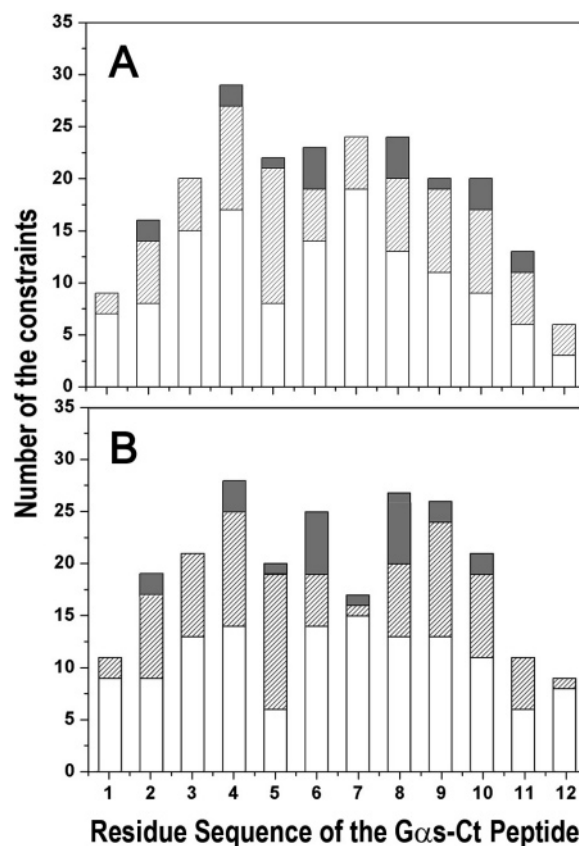


FIGURE 6: Number of constraints per residue for the Gαs-Ct peptide in the absence (A) and presence (B) of the IP iLP1 peptide. Intraresidue, sequential, and medium-range NOEs are shown as white, hatched, and filled bars, respectively.

measurement are two residues at the N- (Ser2) and C-terminal (Val14) positions of the IP iLP1 peptide.

**Description of the 3D Structural Model of the Gαs-Ct Peptide.** On the basis of NOE constraints and dihedral angles, first, 100 first-generation structures for the Gαs-Ct peptide in the absence of the IP iLP1 peptide were obtained using a DGII program calculation. Figure 7E shows the 10 selected structures with a backbone RMSD value of  $1.0 \pm 0.2$  Å for residues Gln2–Leu11. An α-helical structure was clearly observed between residue Gln2 and Leu11, which matched the structural prediction on the basis of the NOE survey data (Figure 5A), and the conformation of residues Gln8–Leu11 was very similar to the α-turn-like structure calculated by Albrizio's group using an 11-residue peptide (16). Then, energy refinement calculations (minimization/dynamic) were carried out on the basis of the best distance geometry structures using a Discover program within the Insight II package. Finally, 11 structures were obtained and superimposed as shown in Figure 7G, in which the backbone RMSD value of the structures (for Gln2–Leu11) was reduced to  $0.7 \pm 0.1$  Å. A similar approach was used to generate the solution structure of the Gαs-Ct peptide in the presence of the IP iLP1 peptide. The 10 selected structures have a backbone RMSD value of  $0.9 \pm 0.1$  Å for Gln2–Gln8 and  $1.5 \pm 0.3$  Å for Tyr 391–Leu394 (Figure 7F). The higher RMSD value in the C-terminal residues indicates that the last four residues are somehow flexible. It was interesting that the α-helical conformation of the C-terminal residues of the free Gαs peptide was destabilized following the



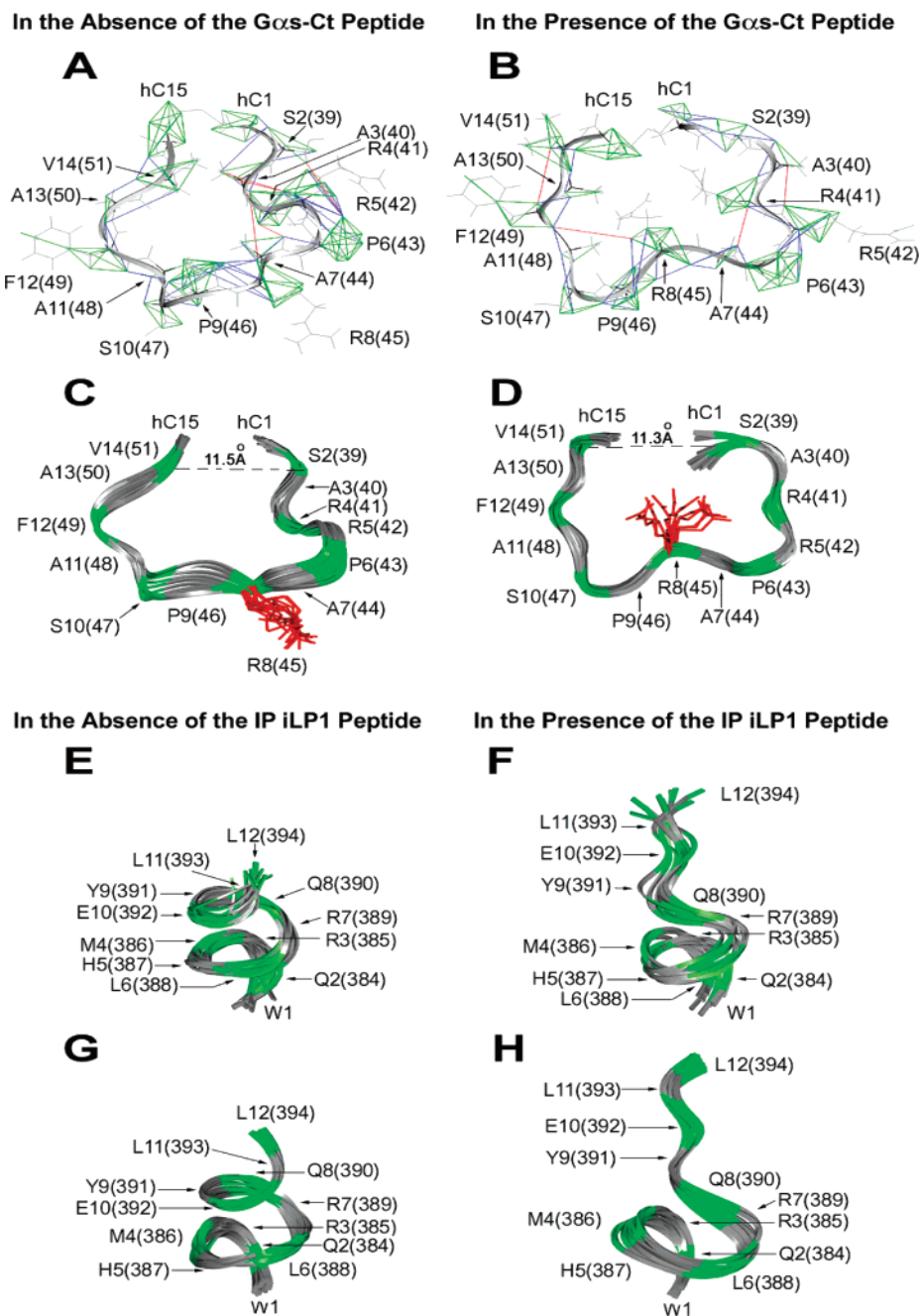


FIGURE 7: The 3D NMR solution structural models for the IP iLP1 and G $\alpha$ s-Ct peptides. The intrasidue (green), sequential (blue), and medium-range (red) NOE distance restraints used to construct the NMR solution structural models of the IP iLP1 peptides in the absence (A) and presence (B) of the G $\alpha$ s-Ct peptides were displayed. The main chains (gray) and side chains (gray) of the IP iLP1 peptides are indicated in a solid rectangular ribbon and stick representations, respectively. Eleven 3D structures (after energy minimization and dynamic refinement) for the IP iLP1 peptides in the absence (C) and presence (D) of the G $\alpha$ s-Ct peptides were superimposed. The main chains (green and gray) of the IP iLP1 molecules and the side chains of Arg8s (red) are indicated in a solid rectangular ribbon and stick representations, respectively. The distances (approximately 11 Å) between the C- and N-termini (excluding the additional hCys as a spacer) of the NMR structures of the IP iLP1 peptides are also displayed. Ten first-generation structures for the G $\alpha$ s-Ct peptides in the absence (E) and presence (F) of the IP iLP1 peptide were superimposed. After energy minimization and dynamic refinement, 11 3D structures for the G $\alpha$ s-Ct peptides in the absence (G) and presence (H) of the IP iLP1 peptide were also superimposed. The amino acid residues (given in single-letter amino acid notation) and numbering within the peptides are shown, and the corresponding sequence numbers in their parent proteins (IP receptor and G $\alpha$ s protein) are indicated in parentheses. All figures were produced using the Insight II package (Accelrys, San Diego, CA).

addition of the IP iLP1 peptide to the solution (Figure 7F,H). This structural change in the C-terminal segment of the G $\alpha$ s protein matched the NOE survey data, in which several  $\alpha$ -helical related NOEs disappeared in the presence of the IP iLP1 peptide (Figure 5B). These observations strongly support that an interaction occurred between the two peptides and that the C-terminal residues of the G $\alpha$ s-Ct peptide were

involved in the interaction with the IP iLP1 peptide in solution.

*Configuration of the NMR Structural Models of IP iLP1 Peptide on the IP Receptor Model.* The NMR solution structural models of the iLP1 peptide were grafted on the IP receptor working model constructed by homology modeling using the crystallographic structure of seven TM domains

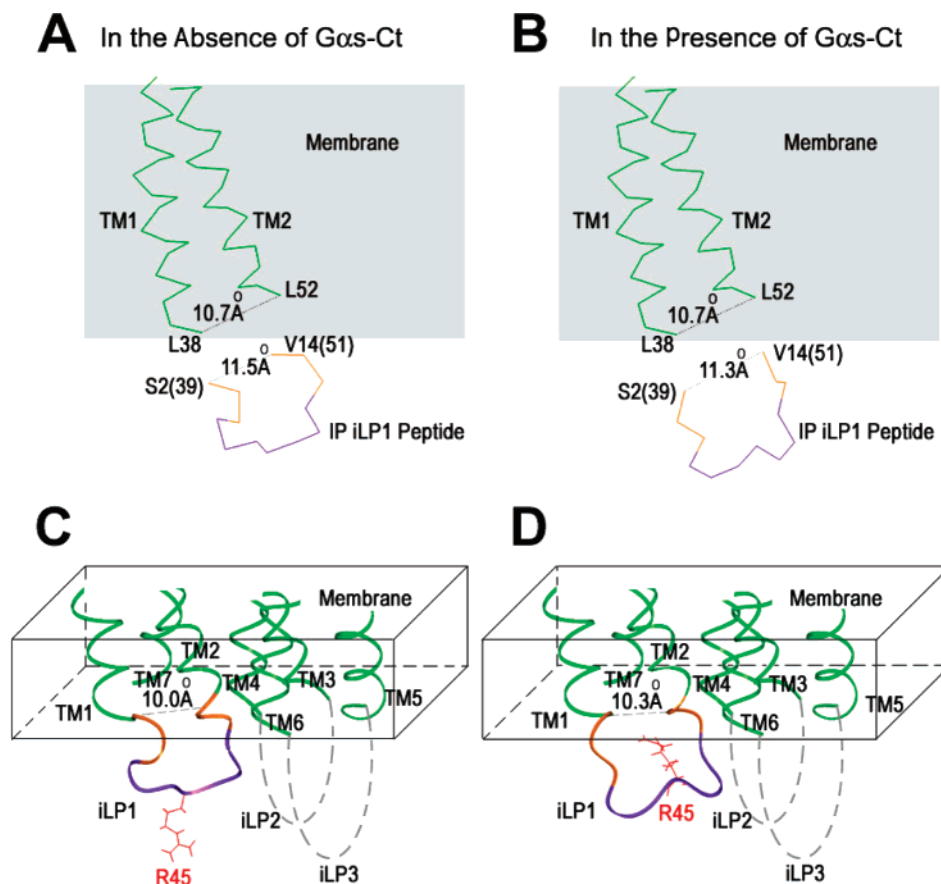


FIGURE 8: Configuration of the NMR structural models of the IP iLP1 peptides to the corresponding TM domains of the IP receptor model. The distance of the TM1 and TM2 of the IP receptor working model generated on the basis of bovine rhodopsin is 10.7 Å (A and B), and the distances between the termini (excluding the hCys as a spacer) of the NMR structural models of the IP iLP1 in the absence (A) and presence (B) of the Gαs Ct peptide are approximately 11 Å. The NMR structures of the IP iLP1 peptides (blue and orange) in the absence (C) and presence (D) of the Gαs Ct peptide were connected to the TM1 and TM2 (green) of the IP receptor working model with the common trans peptide bond. Energy minimizations were then performed for the connected molecules. The distances between the TM1s and TM2s that connected the iLP1s in the IP receptor models were not significantly altered. The positions of the seven residues (blue) involved in the IP signaling identified previously (21) are also highlighted. However, the conformations of the side chains of residue Arg45s (corresponding to Arg8s in the IP iLP1 peptide, red) have significantly been altered by the comparison of the conformations in the absence (C) and presence (D) of the Gαs-Ct peptide. The dashed lines denote the undefined structures of the second and (iLP2) and third (iLP3) intracellular loops.

of bovine rhodopsin as a template (19, Figure 1A). The configuration of the IP iLP1 structure on the IP seven TM model was achieved without further modification of the NMR solution structure because the distance between the N- and C-termini of the peptide shown in the NMR structure is approximately 11 Å (Figure 7C,D), which could be fitted onto the separation (approximately 10.7 Å) between the Cα atoms of Leu38 in the first (TM1) and Leu52 in the second (TM2) TM domains, which are the residues flanking the N- and C-termini of the IP iLP1 domain (Figure 8A,B). The steps of the configuration were performed as follows: first, by placing the N- and C-termini of the NMR structure of the IP iLP1 peptide onto the C- and N-termini of the TM1 and TM2 helices; second, by matching the distance between the TM1 and TM2 with the distances between the N- and C-termini of the peptide (Figure 8A,B); third, by forming covalent bonds between the TM domains and the iLP1 with a common trans conformation; fourth, by subjecting the connected molecule to energy minimization in order to obtain a final conformation. Finally, the configuration was satisfactorily evaluated for having no major bond violations and for having minimal conformational changes in comparison to the configurations of the NMR iLP1 structures (Figure

8C,D). In this structural study, the major difference of the side chain orientation of Arg45 in the IP iLP1 in the absence and presence of the Gαs-Ct peptide was clearly identified (Figure 8C,D). This observation suggests that the Arg45 residue may play an important role in the interaction with the Gαs-Ct peptide.

*Comparison of the NMR Structural Models of the Gαs-Ct Peptide and the Crystal Structure of the C-Terminal Segment of Gαs Protein.* The NMR solution structural models of the Gαs-Ct peptide in the absence and presence of the IP iLP1 peptide were superimposed to the crystal structure of the human Gαs protein (14, Figure 9). Residues E392 through L394 are disordered at the C-terminal domain of the crystal structure (Figure 1E). The NMR solution structures of the N-terminal residues (Q384–R389) of the Gαs-Ct peptide in the absence (Figure 9A) and presence (Figure 9B) of the IP iLP1 peptide showed similar helical structures with the corresponding position of the crystal structure. The backbone RMSD for the superimposed eight residues between the NMR and crystal structures is approximately 1.5 Å. In addition, the NMR solution structure studies could be used to predict and display the conformation of the C-terminal residues (Q390–E392) of the Gαs protein,



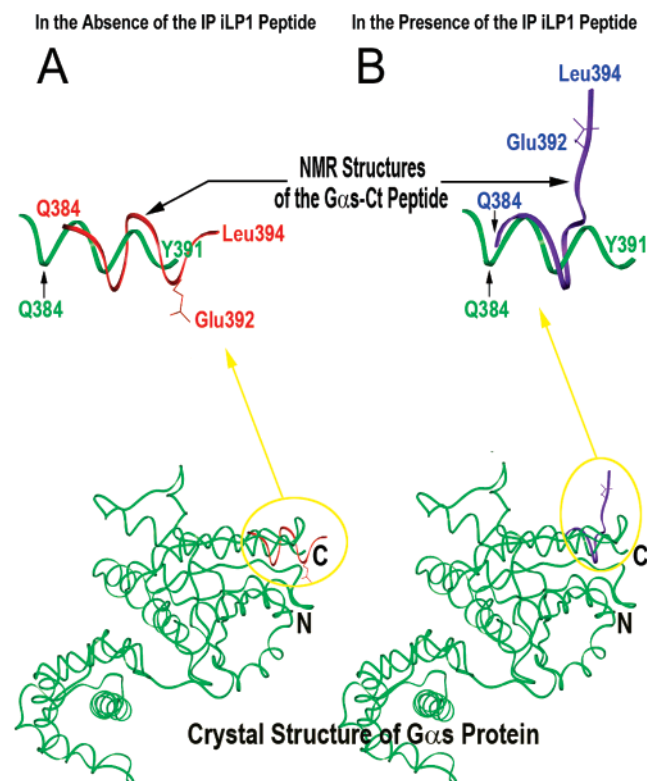


FIGURE 9: Superimposition of the NMR structural models of the G $\alpha$ s-Ct peptides on the crystal structure of the G $\alpha$ s protein. The NMR structural models of the G $\alpha$ s-Ct peptides in the absence (A, red) and presence (B, purple) of the IP iLP1 peptide were superimposed to the crystal structure (14; green) of the human G $\alpha$ s protein. The side chain of residue Glu394 was indicated.

which assumes an  $\alpha$ -helical conformation in the absence of the IP iLP1 peptide (Figure 9A). Moreover, the helical structure may be unwound in the presence of the IP iLP1 peptide (Figure 9B). This conformational change reflected the dynamic feature of the C-terminal residues in the interaction with GPCR.

## DISCUSSION

Synthetic peptides have been used as important tools in mimicking functional domains of receptors, including GPCRs (33–37). It shall be indicated that the implication of the peptide studies for the protein needs to be considered with the corresponding protein backbones. The models of the solution structure of the constrained peptide that mimics the IP iLP1 and the peptide that mimics the G $\alpha$ s C-terminal domain should agree with the backbone folding of their parent protein. Thus, the configuration of the 3D solution structure of the IP iLP1 to the TM domain model of the IP receptor (Figure 8) and the superimposed solution structure of the G $\alpha$ s-Ct with the crystal structure of the G $\alpha$ s protein (Figure 9) are important steps in showing the reliability of peptide studies using high-resolution NMR spectroscopy. The loop structures with two turns observed in the NMR structures of the IP iLP1 peptides that fit perfectly with the separation distance between the TM1 and TM2 of the receptor model have provided important evidence for a reasonable configuration of the particular domain of the protein. On the other hand, the limited variation of the backbone structures of the C-terminal segments between the

crystal structure and NMR solution structure in the N-terminal segment (Q384–R389) of the G $\alpha$ s-Ct peptide also indicated that the NMR assignment is within a range with only a small variation. In addition, the NMR structural studies using a mixture of the IP iLP1 and G $\alpha$ s-Ct peptides in solution allowed for the understanding of their dynamic interaction with each other, which is difficult to be achieved by crystal structural studies. Therefore, the NMR solution structures of the IP iLP1 and G $\alpha$ s-Ct peptides described in this paper represent an important initial step toward the characterization of receptor/G protein interactions on a structural level in solution.

In a previous report, we have identified that the mutation at Arg60 in the iLP1 of the TP receptor impaired the receptor's signal transduction (26). It is interesting that the basic residues in the iLP1s of the eight prostanoid receptors are highly conserved even though they mediate diverse and opposing signaling pathways. Recently, we have also identified that six additional residues surrounding the conserved Arg45 in the IP iLP1 are also involved in the receptor signaling (24). To understand the structure/function relationship, it is important to gain structural information for the intracellular domain of the IP iLP1 and the coupling site of the G protein. The information obtained from the current studies is able to address several important structure/function relationships of the IP iLP1 involved in the receptor signaling: (1) The seven residues that influence the G $\alpha$ s protein coupling, recently identified by NMR and site-directed mutagenesis studies (24), are localized within the loop with two turn structures in the IP iLP1 (Figure 7C,D). (2) The two Pro residues (Pro43 and Pro46) near Arg45 are important in the formation of the two turn structures (Figure 7A,B). The molecular mechanism of the mutations of the Pro residues (Pro43 or Pro46) destroying the receptor signaling described in the previous paper (24) could be the alternation of the turn structures by the replacement of either Pro residue. (3) The charge contact could be important to the receptor/G protein coupling in the iLP1 domain of the IP receptor and the C-terminal region of the G $\alpha$ s, which was supported by the observation of the conformational change of the side chain of Arg45 (Figure 7C,D) in the IP iLP1 peptide upon interaction with the G $\alpha$ s-Ct peptide. (4) On the basis of the observation of some weak intermolecular NOEs, we tentatively put forward the idea that there probably exists a charge contact between Arg45 of the IP receptor and Glu392 of the G $\alpha$ s C-terminal segment and/or a hydrophobic contact between Pro43 or Pro46 of the IP receptor and Leu393-Leu394 of the G $\alpha$ s C-terminal segment. But we could not exclude other possible contacts between the IP iLP1 and G $\alpha$ s-Ct (Table 3). (5) The main difference in the structure of the IP iLP1 domain may not be the structure itself, but a reorientation of an arginine (Arg45) side chain from an outward pointing position to an inward (toward the putative TM helix space) orientation (Figure 8C,D), probably with a concomitant exposure of a glutamic acid (Glu392) in the G $\alpha$ s-Ct peptide through straightening the C-terminal  $\alpha$ -helix structure if the orientation of the G $\alpha$ s-Ct peptide was correctly predicted (Figure 9). It should also be pointed out that the bioactive conformation of a flexible peptide does not necessarily correspond to the one prevailing in solution. Further studies to confirm the residues in the C-terminal segment of the G $\alpha$ s protein important to the Gs-

Table 3: Possible Intermolecular NOEs between the IP iLP1 Peptide and the G $\alpha$ s-Ct Peptide<sup>a</sup>

possible inter-molecular NOEs	dimension 1		dimension 2		possible forces contributing to interactions
	ppm	assigned protons in IP iLP1 peptide	ppm	assigned protons in G $\alpha$ s-Ct peptide	
1	1.549	Arg8(45): $\gamma$ H	2.271	Glu10(392): $\gamma$ H	charge
2	1.538	Arg8(45): $\gamma$ H	2.271	Glu10(392): $\gamma$ H	contact
3	1.856	Pro6(43): $\beta$ H	0.795	Leu11(393): $\delta$ H	hydrophobic
4	1.868	Pro9(46): $\beta$ H	0.795	Leu11(393): $\delta$ H	contact

<sup>a</sup> The weak NOEs were observed from the NOESY spectrum for the mixture of the IP iLP1 peptide (5.4 mM) and the G $\alpha$ s-Ct peptide (8.4 mM). The amino acid residue numbering for the peptides is shown, and the corresponding residue numbers in their parent proteins (the IP receptor and the G $\alpha$ s protein) are indicated in parentheses.

mediated signaling will help to settle the hypothesis.

The NMR structures of the IP iLP1 can be used to guide mutagenesis studies and protein designs for the IP receptor and other prostanoid receptors because the Arg45 residue is highly conserved with Arg or Lys in the other prostanoid receptors (24). The fact that both Arg45 in the IP iLP1 (24) and Arg60 in the TP iLP1 (26) are involved in different signaling mediated by the different Gs and Gq protein couplings, respectively, has suggested that the positive charge of the basic residues in the iLP1 positions of other prostanoid receptors could possibly have general contacts with their specific G proteins. However, the identified six residues surrounding Arg45 in the IP iLP1 involved in G $\alpha$ s coupling are not very conserved. Therefore, they might be important players in the determination of the conformations of the iLP1s in the different prostanoid receptors coupled to their specific G proteins.

## ACKNOWLEDGMENT

We thank Drs. Xialian Gao and Youlin Xia in the Chemistry Department at The University of Houston for access to the NMR facility and for providing valuable advice on taking the NMR spectra. We also thank Vanessa Cervantes and Sam Li for manuscript preparation assistance.

## REFERENCES

- Katsuyama, M., Sugimoto, Y., Namba, T., Irie, A., Negishi, M., Narumiya, S., and Ichikawa, A. (1994) Cloning and expression of a cDNA for the human prostacyclin receptor, *FEBS Lett.* **344**, 74–88.
- Abramovitz, M., Boie, Y., Nguyen, T., Rushmore, T. H., Bayne, M. A., Metters, K. M., Slipetz, D. M., and Grygorczyk, R. (1994) Cloning and expression of a cDNA for the human prostanoid FP receptor, *J. Biol. Chem.* **269**, 2632–2636.
- Funk, C. D., Furci, L., FitzGerald, G. A., Grygorczyk, R., Rochette, C., Bayne, M. A., Abramovitz, M., Adam, M., and Metters, K. M. (1993) Cloning and expression of a cDNA for the human prostaglandin E receptor EP<sub>1</sub> subtype, *J. Biol. Chem.* **268**, 26767–26772.
- An, S., Yang, J., Xia, M., and Goetzl, E. J. (1993) Cloning and expression of the EP<sub>2</sub> subtype of human receptors for prostaglandin E<sub>2</sub>, *Biochem. Biophys. Res. Commun.* **197**, 263–270.
- Bastien, L., Sawyer, N., Grygorczyk, R., Metters, M., and Adam, M. (1994) Cloning, functional expression, and characterization of the human prostaglandin E<sub>2</sub> receptor EP<sub>2</sub> subtype, *J. Biol. Chem.* **269**, 11873–11877.
- Adam, M., Boie, Y., Rushmore, T. H., Muller, G., Bastien, L., McKee, K. T., Metters, K. M., and Abramovitz, M. (1994) Cloning and expression of three isoforms of the human EP<sub>3</sub> prostanoid receptor, *FEBS Lett.* **338**, 170–174.
- Regan, J. W., Bailey, T. J., Donello, J. E., Pierce, K. L., Pepperi, D. J., Zhang, D., Kedzie, K. M., Fairbairn, C. D., Bogardus, A. M., Woodward, D. F., and Gil, D. W. (1994) Molecular cloning and expression of human EP<sub>3</sub> receptors: evidence of three variants with differing carboxyl termini, *Br. J. Pharmacol.* **111**, 377–385.
- Kunapuli, S. P., Mao, G. F., Bastepe, M., Liu-Chen, L.-Y., Li, S., Cheung, P. P., DeRiel, J. K., and Ashby, B. (1994) Cloning and expression of a prostaglandin E receptor EP<sub>3</sub> subtype from human erythroleukaemia cells, *Biochem. J.* **298**, 263–267.
- Yang, J., Xia, M., Goetzl, E. J., and An, S. (1994) Cloning and expression of the EP<sub>3</sub>-subtype of human receptors for prostaglandin E<sub>2</sub>, *Biochem. Biophys. Res. Commun.* **198**, 999–1006.
- Hamm, H. E., Deretic, D., Arendt, A., Hargrave, P. A., Koenig, B., and Hofmann, K. P. (1998) Site of G protein binding to rhodopsin mapped with synthetic peptides from the alpha subunit, *Science* **241**, 832–835.
- Gether, U. (2000) Uncovering molecular mechanisms involved in activation of G protein-coupled receptors, *Endocr. Rev.* **21**, 90–113.
- Albrizio, S., Caliendo, G., D'errico, G., Novellino, E., Rovero, P., and D'ursi, A. M. (2005) Galpha(s) protein C-terminal alpha-helix at the interface: does the plasma membrane play a critical role in the Galpha(s) protein functionality?, *J. Pept. Sci.* **11**, 617–626.
- Benjamin, D. R., Markby, D. W., Bourne, H. R., and Kuntz, I. D. (1995) Solution structure of the GTPase activating domain of alphas, *J. Mol. Biol.* **254**, 681–691.
- Sunahara, R. K., Tesmer, J. J., Gilman, A. G., and Sprang, S. R. (1997) Crystal structure of the adenylyl cyclase activator Gsalpha, *Science* **278**, 1943–1947.
- Dursi, A. M., Albrizio, S., Greco, G., Mazzeo, S., Mazzoni, M. R., Novellino, E., and Rovero, P. (2002) Conformational analysis of the Galpha(s) protein C-terminal region, *J. Pept. Sci.* **8**, 476–488.
- Albrizio, S., D'ursi, A., Fattorusso, C., Galoppini, C., Greco, G., Mazzoni, M. R., Novellino, E., and Rovero, P. (2000) Conformational studies on a synthetic C-terminal fragment of the alpha subunit of G(s) proteins, *Biopolymers* **54**, 186–194.
- Mazzoni, M. R., Taddei, S., Giusti, L., Rovero, P., Galoppini, C., D'ursi, A., Albrizio, S., Triolo, A., Novellino, E., Greco, G., Lucacchini, A., and Hamm, H. E. (2000) A galpha(s) carboxyl-terminal peptide prevents G(s) activation by the A(2A) adenosine receptor, *Mol. Pharmacol.* **58**, 226–236.
- Pellegrini, M., and Mierke, D. F. (1999) Structural characterization of peptide hormone/receptor interactions by NMR spectroscopy, *Biopolymers* **51**, 208–220.
- Wand, A. J., and Englander, S. W. (1996) Protein complexes studied by NMR spectroscopy, *Curr. Opin. Biotechnol.* **7**, 403–408.
- Ruan, K. H., Wu, J., So, S. P., Jenkins, L. A., and Ruan, C. H. (2004) NMR structure of the thromboxane A<sub>2</sub> receptor ligand recognition pocket, *Eur. J. Biochem.* **271**, 3006–3016.
- Wu, J., So, S. P., and Ruan, K. H. (2003) Solution structure of the third extracellular loop of human thromboxane A<sub>2</sub> receptor, *Arch. Biochem. Biophys.* **414**, 287–293.
- So, S. P., Wu, J., Huang, G., Huang, A., Li, D., and Ruan, K. H. (2003) Identification of residues important for ligand binding of thromboxane A<sub>2</sub> receptor in the second extracellular loop using the NMR experiment-guided mutagenesis approach, *J. Biol. Chem.* **278**, 10922–10927.
- Ruan, K. H., Wu, J., So, S. P., and Jenkins, L. A. (2003) Evidence of the residues involved in ligand recognition in the second extracellular loop of the prostacyclin receptor characterized by high resolution 2D NMR techniques, *Arch. Biochem. Biophys.* **418**, 25–33.
- Zhang, L., Huang, G., Wu, J., and Ruan, K. H. (2005) A profile of the residues in the first intracellular loop critical for Gs mediated signaling of human prostacyclin receptor characterized by an integrative approach of NMR-experiment and mutagenesis, *Biochemistry* **44**, 11389–11401.
- Wüthrich, K. (1986) *NMR of Proteins and Nucleic Acids*, Wiley, New York.
- Geng, L., Wu, J., So, S. P., Huang, G., and Ruan, K. H. (2004) Structural and functional characterization of the first intracellular loop of human thromboxane A<sub>2</sub> receptor, *Arch. Biochem. Biophys.* **423**, 253–265.
- Wüthrich, K., Billeter, M., and Braun, W. (1983) Pseudo-structures for the 20 common amino acids for use in studies of protein conformations by measurements of intramolecular proton–proton

- distance constraints with nuclear magnetic resonance, *J. Mol. Biol.* 169, 949–961.
28. Masters, S. B., Sullivan, K. A., Miller, R. T., Beiderman, B., Lopez, N. G., Ramachandran, J., and Bourne, H. R. (1988) Carboxyl terminal domain of Gs  $\alpha$  specifies coupling of receptors to stimulation of adenylyl cyclase, *Science* 241, 448–451.
29. Rasenick, M. M., Watanabe, M., Lazarevic, M. B., Hatta, S., and Hamm, H. E. (1994) Synthetic peptides as probes for G protein function. Carboxyl-terminal G  $\alpha$  s peptides mimic Gs and evoke high affinity agonist binding to beta-adrenergic receptors, *J. Biol. Chem.* 269, 21519–21525.
30. Feldman, D. S., Zamah, A. M., Pierce, K. L., Miller, W. E., Kelly, F., Rapacciuolo, A., Rockman, H. A., Koch, W. J., and Luttrell, L. M. (2002) Selective inhibition of heterotrimeric Gs signaling. Targeting the receptor-G protein interface using a peptide minigene encoding the G $\alpha$ (s) carboxyl terminus, *J. Biol. Chem.* 277, 28631–28640.
31. Gilchrist, A., Bunemann, M., Li, A., Hosey, M. M., and Hamm, H. E. (1999) Selective inhibition of heterotrimeric Gs signaling. Targeting the receptor-G protein interface using a peptide minigene encoding the G $\alpha$ (s) carboxyl terminus, *J. Biol. Chem.* 274, 6610–6616.
32. Mazzoni, M. R., Taddei, S., Giusti, L., Rovero, P., Galoppini, C., D'Ursi, A., Albrizio, S., Triolo, A., Novellino, E., Greco, G., Lucacchini, A., and Hamm, H. E. (2000) A galpha(s) carboxyl-terminal peptide prevents G(s) activation by the A(2A) adenosine receptor, *Mol. Pharmacol.* 58, 226–236.
33. Franzoni, L., Nicastro, G., Pertinhez, T. A., Tato, M., Nakaie, C. R., Paiva, A. C., Schreiner, S., and Spisni, A. (1997) Structure of the C-terminal fragment 300–320 of the rat angiotensin II AT(1A) receptor and its relevance with respect to G-protein coupling, *J. Biol. Chem.* 272, 9734–9741.
34. Anand-Srivastava, M. B., Sehl, P. D., and Lowe, D. G. (1996) Cytoplasmic domain of natriuretic peptide receptor-C inhibits adenylyl cyclase. Involvement of a pertussis toxin-sensitive G protein, *J. Biol. Chem.* 271, 19324–19329.
35. Grasso, P., Leng, N., and Reichert, L. E., Jr. (1995) A synthetic peptide corresponding to residues 645–653 in the carboxyl terminal cytoplasmic domain of the rat testicular follicle stimulating hormone receptor modulates G protein coupled-receptor signaling in rat testis membranes and in intact cultured rat Sertoli cells, *Mol. Cell. Endocrinol.* 108, 43–50.
36. Dias, J. A. (1996) Human follitropin heterodimerization and receptor binding structural motifs: identification and analysis by a combination of synthetic peptide and mutagenesis approaches, *Mol. Cell. Endocrinol.* 125, 45–54.
37. Kole, H. K., Liotta, A. S., Kole, S., Roth, J., Montrose-Rafizadeh, C., and Bernier, M. (1996) A synthetic peptide derived from a COOH-terminal domain of the insulin receptor specifically enhances insulin receptor signaling, *J. Biol. Chem.* 271, 31619–31626.

BI0515669